



Published in final edited form as:

Cancer Immunol Immunother. 2008 July ; 57(7): 1017–1027. doi:10.1007/s00262-007-0433-x.

A33 antigen displays persistent surface expression

Margaret E. Ackerman,

Department of Biology, Massachusetts Institute of Technology, Cambridge, USA

Cecile Chalouni,

Department of Cell Biology, Ludwig Institute for Cancer Research, Yale University School of Medicine, New Haven, USA

Michael M. Schmidt,

Department of Biological Engineering, Massachusetts Institute of Technology, Bldg E19-551, 50 Ames Street, Cambridge, MA 02139, USA

Vivek V. Raman,

Department of Biological Engineering, Massachusetts Institute of Technology, Bldg E19-551, 50 Ames Street, Cambridge, MA 02139, USA

Gerd Ritter,

Ludwig Institute for Cancer Research, New York Branch, Memorial Sloan-Kettering Cancer Center, New York, USA

Lloyd J. Old,

Ludwig Institute for Cancer Research, New York Branch, Memorial Sloan-Kettering Cancer Center, New York, USA

Ira Mellman, and

Department of Cell Biology, Ludwig Institute for Cancer Research, Yale University School of Medicine, New Haven, USA

K. Dane Wittrup

Department of Biological Engineering, Massachusetts Institute of Technology, Bldg E19-551, 50 Ames Street, Cambridge, MA 02139, USA

Department of Chemical Engineering, Massachusetts Institute of Technology, Bldg E19-551, 50 Ames Street, Cambridge, MA 02139, USA

K. Dane Wittrup: wittrup@mit.edu

Abstract

The A33 antigen is a cell surface glycoprotein of the small intestine and colonic epithelium with homology to tight junction-associated proteins of the immunoglobulin superfamily, including CAR and JAM. Its restricted tissue localization and high level of expression have led to its use as a target in colon cancer immunotherapy. Although the antigen is also present in normal intestine, radiolabeled antibodies against A33 are selectively retained by tumors in the gut as well as in metastatic lesions for as long as 6 weeks. Accordingly, we have studied the trafficking and kinetic properties of the antigen to determine its promise in two-step, pretargeted therapies. The localization, mobility, and persistence of the antigen were investigated, and this work has demonstrated that the antigen is both highly immobile and extremely persistent—retaining its surface localization for a turnover half-life of greater than 2 days. In order to explain these unusual properties, we explored the possibility that

A33 is a component of the tight junction. The simple property of surface persistence, described here, may contribute to the prolonged retention of the clinically administered antibodies, and their uncommon ability to penetrate solid tumors.

Keywords

A33 antigen; Radioimmunotherapy; Colon cancer; Tight junction; Immunoglobulin superfamily

Introduction

The recent success of several radioimmunotherapeutics has demonstrated proof of principle for this type of targeted cancer therapy [1]. Unfortunately, in many potential applications, bone marrow toxicity limits therapy. In order to circumvent this toxicity, a two-step strategy, known as pretargeted immunotherapy (PRIT) has been proposed, in which the targeting construct and radionuclide are separated into two distinct dosing steps. In this way, one preserves the specificity of antibody binding in tumor targeting, but eliminates the toxic effects of long-lived directly labeled antibodies. When compared to single step therapies using directly labeled antibodies, PRIT has generally lead to lower toxicity and better efficacy [2–4]. However, the addition of a separate step constrains the desirable kinetic attributes of the cellular target in comparison with direct RIT, immunotoxin therapy, or approaches relying on effector functions. In PRIT, the competing interests of target saturation, clearance of unbound construct from the circulation, availability of the construct to chelated radionuclide, sufficient proximity to the nucleus relative to decay pathlength, and the half-life of the radionuclide must all be taken into consideration. This study seeks to determine if the A33 antigen, a member of the immunoglobulin superfamily (IGSF) with homology to cell adhesion [5] and tight junction-associated (TJ) proteins [6], possesses the properties particularly suited for PRIT.

The A33 antigen is an abundant cell surface protein expressed in 95% of colon tumors, and in normal intestine, but not in other organs [7]. This restricted expression pattern led to interest in use of the A33 antigen in RIT, and directly $^{125/131}\text{I}$ radiolabeled A33 antibodies were administered to patients with colon cancer in a series of phase I and II clinical trials [8–13]. The results of these trials were mixed from a therapeutic perspective, as some patients developed an anti-antibody response [14], and there was dose-limiting bone marrow toxicity. However, they were also quite promising in that they exhibited a startlingly localized persistence of radiolabel. A33 was constitutively expressed in the entire intestine, and evenly throughout the villus axis [15]. Provocatively, however, it was found that after an initial period of time in which the therapeutic conjugate bound the entire intestine, after a period of a week, staining was present only in tumors—both primary and metastatic sites [8]—and whole body scans revealed labeling even 6 weeks after antibody administration [10].

Distinguishing self from target cells poses a particular problem in cancer, in which the tumor cells are of self-origin and consequently share much antigenic similarity with the tissue of their origin. RIT rests on the premise that there are surface antigens with differential expression in tumors. Despite failing to fulfill this basic premise, and consequent dosing of the entire intestine with radioactivity in A33 antigen RIT studies, dose-limiting toxicities were not gastrointestinal. This lack of gastrointestinal toxicity could be attributed to the relatively small dose of radiation to both tumor and normal intestine in comparison to the dose absorbed by the bone marrow, which was the limiting toxicity. Under conditions in which a therapeutic effect on tumor cells is achieved, it is likely that the expression on normal cells will present a toxicity problem. Accordingly, the presumptive ceiling imposed by normal tissue expression, and the tumor-specific staining observed after a week, provoke considerable interest in the study of A33 as a two-step immunotherapy target.

Several possible explanations have been advanced as to how tumor specificity occurs for A33 antibodies, including differential accessibility or endocytosis between normal and cancerous tissue. However, the simplest notion is that specificity results from normal shedding of the colonic epithelium. As this process of migration and sloughing occurs over the course of several days, this theory is consistent with the clinical data.

Regardless of the mechanism by which tumor-specificity is gained, in order to be a useful target in PRIT, the antibody specifically localized to tumors after 1 week must be retained on the tumor cell surface—available to bind a radionuclide construct. Therefore, we undertook a study to determine the trafficking and persistence of the A33 antigen in cultured colon tumor cell lines, as well as some preliminary work to understand the etiology of this unique in vivo persistence.

Materials and methods

Cell culture

The immortalized human colonic tumor cell lines LS174T, LIM1215, COLO205, and SW1222 cells were grown in advanced MEM supplemented with L-glutamine and 10% FBS (Gibco). Where appropriate, cells were fixed and permeabilized with BD cytofix and cytoperm (BD Biosciences) according to the manufacturer's instructions. For internalization studies, latrunculin B (Sigma) and nocodazole (Sigma) were dissolved in DMSO and added to culture media for final concentrations of 100 nM and 50 μ M, respectively. EGTA was directly dissolved in culture media for a final concentration of 25 mM. MCF-7 cells expressing a CEACAM1-egfp fusion protein used in photobleaching experiments were a kind gift of Dr. John Shively and were cultured as described previously [16].

Fluorescent labeling of cells

The mouse anti-A33 antibody m100.310 (gift of Dr. Gerd Ritter) was conjugated to Alexa*488 or fluorescein according to the manufacturer's instructions (Molecular Probes A-20181, F-6433), and goat anti-mouse PE was used as a secondary (Sigma). Anti-CEA sHMF was likewise conjugated to Alexa*594 (Molecular Probes A30008). For colocalization experiments, LIM1215 cells were permeabilized-fixed with methanol at -20°C for 5 min, and then stained with either rabbit anti-human occludin (Zymed), or mouse anti-human ZO-1 (Zymed). These primary antibodies were subsequently detected by Cy3-conjugated donkey anti-rabbit and anti-mouse antibodies, respectively (Jackson immunoresearch Laboratories). Actin was labeled with Alexa*546-conjugated phalloidin (Molecular Probes).

Vybrant DiI (Molecular Probes) was used to label bulk membrane for photobleaching experiments. For DiI labeling, the media above the monolayer was replaced with 300 mM sucrose in PBS, and then 2 μ l of the DiI label was slowly added to the sucrose solution above the monolayer and allowed to incorporate into the membrane for 10 min before the sucrose solution was removed and replaced by fresh media.

Fluorescence microscopy

Cells were grown on coverslip-bottomed dishes (Mattek), labeled as described above, and imaged on a Deltavision deconvolution microscope with a 1.4 NA oil lens at 100 \times magnification. The resulting images were subsequently deconvolved and analyzed using the SoftWorx application.

Colocalization study images were acquired using a confocal LSM510 Zeiss microscope equipped with an oil immersion plan apochromatic 100 \times lens, NA 1.4.

Flow cytometric internalization assay

For analysis of kinetic internalization of the antigen in live cells, a suspension of 4×10^6 cells/ml was labeled with m100.310 Alexa*488 in media on ice for 1 h at 100 ng/ml in order to identify total surface-localized antigen. After labeling, cells were washed and resuspended in CO₂-independent media (Gibco), diluted to 4×10^5 cells/ml, and incubated in a 37°C shaker in air for the course of the experiment. At each timepoint, 1 ml aliquots were taken, washed once with 0.5 ml PBS 0.1% BSA, and incubated with 100 µl of 2:100 dilution of anti-mouse PE (Sigma) on ice for 15 min, allowing for the quantification of antigen that remained surface-localized after the incubation period. Cellular fluorescence was then analyzed on a Beckman Coulter XL-4 Xow cytometer. Secondary-only and 4°C controls were maintained.

Transepithelial electrical resistance measurements

Eighty thousand SW1222 cells were plated on a transwell insert (Corning 3470). One day after plating, 1 µl of anti-FLAG antibody (Sigma) and huA33 antibody (gift of Dr. Gerd Ritter) at 1 mg/ml were added to both apical and basolateral chambers. Each day following antibody addition, resistance measurements were taken with a millcell-ERS (Millipore) after equilibration of the plate for an hour at room temperature.

Fluorescence recovery after photobleaching

LS174T cells were labeled with either fluoresceinated m100.310 or the membrane dye DiI as described above. Bleaches were performed on a Zeiss LSM 510 confocal microscope with a 1.4 NA oil lens at 67× magnification on a heated stage. Sections of membrane were bleached with full laser power on all channels for 50–100 iterations, resulting in bleaches of between 20 and 80% of initial fluorescence. Fluorescence intensity in the bleach region was recorded and then adjusted to correct for background bleaching due to repetitive imaging over the course of the experiment. Appropriate controls were performed in order to ensure that bleaching was non-reversible. The data presented is the average of a minimum of six experiments. The resulting fluorescence recovery data was used to calculate relative diffusivities [17–19].

Biotinylation turnover assay

The biotinylation turnover assay was adapted from a protocol designed to measure endocytosis and recycling rates [20]. Briefly, cells were cultured in 12 well dishes overnight, then cell surface proteins were pulse biotinylated by incubation in 1 ml of ice cold PBS containing freshly dissolved NHS-SS-Biotin (Pierce 21217) for 1 h. Following this incubation media was replaced with 100 mM Tris to quench unreacted biotin for 5 min at 4°C. After quenching, the Tris solution was removed and replaced with media, and cells were returned to the incubator at 37°C and 5% CO₂. At each timepoint, media was removed and cells were incubated in 1 ml lysis buffer for 10 min. They were washed off the plate and set on ice in a microfuge tube for another 10 min after vortexing briefly. Samples were then spun at 12,000 rpm for 15 min to clear the lysate, which was then frozen. When the timecourse was complete, the lysates were incubated with 100 µl streptavidin resin beads (Pierce 53114) on a rotator overnight at 4°C. The streptavidin beads were then spun down, washed, and the bound biotinylated proteins were released by incubation in 75 µl of 100 mM DTT in PBS at 37°C for 1 h, mixing every 15 min. Samples were then mixed with loading buffer and run on a 4–12% bis-tris gel (Invitrogen) and run and transferred onto nitrocellulose according the manufacturer's instructions. The nitrocellulose membrane was blocked and blotted as previously described to detect denatured A33 antigen [21].

Results

A panel of A33-expressing colon tumor cell lines were fixed, permeabilized, and stained to detect A33 (Fig. 1a). There was very little evidence of intracellular staining in three of the four cell lines tested, suggesting there may be little, if any, constitutive endocytosis of the A33 antigen. Additionally, live cells were incubated with antibody for various and extended periods of time, in order to follow antibody-driven internalization, the same pattern of membrane-only staining was observed (data not shown) in these cell lines. This result contrasts earlier reports in which acid washes of labeled SW1222 cells demonstrated the internalization of 40% of the antigen when complexed with an antibody that recognizes a different epitope [22]. This discrepancy between our findings using SW1222 and previous studies may be due to differences in the methodologies used to identify surface and intracellular pools, or to a differential effect of the two anti-A33 antibodies on antigen trafficking. LIM1215 cells were an exception and had clear intracellular accumulation, both in fixed cells and in live antibody-complexed populations. This cell line may be representative of a subclass of colonic crypt cells located at the extreme tip of the villus, which are proximal to being shed (C. Chalouni, unpublished).

These localization patterns were confirmed and quantified for a larger population of cells using a kinetic flow cytometry assay (M. Schmidt, in preparation) capable of following the course of antigen internalization (Fig. 1b). Suspended cells were A33-labeled on ice, washed, and incubated in media at 37°C. At various times, aliquots were removed and labeled with PE-conjugated anti-mouse secondary, such that primary signal corresponds to total antibody-labeled antigen, and secondary signal to the fraction of labeled antigen that remains surface accessible. Average fluorescence intensities were standardized to time zero and graphed over time. In most cell lines, the fractional decline in primary and secondary signals was roughly equal, indicating that the bulk of the primary-labeled antigen remained on the cell surface, accessible to secondary. In each experiment, primary signal was seen to decrease, which is likely due to dissociation of the primary antibody, as the antigen itself is not shed [8]. However, the possibility that there is rapid catabolism of antibody following internalization has not been eliminated.

Overall, with the exception of LIM1215, there appeared to be little endocytosis in the cell lines tested (Fig. 1b). Despite the limitations inherent to assaying cells in suspension, and the significant decrease in primary signal over the course of the experiment, these results are consistent with the small amount of A33 observed intracellularly in cultured monolayers both at steady state (Fig. 1a) and when complexed with m100–310 antibody for a prolonged period of time (data not shown), as well as in resected human colon.

The lack of significant internalization of the antigen in several tumor cell lines raised questions concerning the mechanism of this persistence at the surface. Given its homology to several tight junction-associated proteins and cell adhesion molecules (CAMs), a series of colocalization studies were performed (Fig. 2). Despite differing substantially from the other lines tested, LIM1215 cells were used for this work, as they were potentially more discriminatory due to their internal reservoir of antigen. Indeed, in immunofluorescence images of LIM1215 cells, A33 was shown to partially colocalize with occludin (2a), ZO-1 (2b), and actin (2c), not only at the plasma membrane, but also in a few intracellular vesicles.

Next, based on its homology to and partial colocalization with various TJ proteins, we determined whether A33 is trafficked in a manner similar to other TJ proteins. A number of physiological changes and signaling molecules are capable of altering the composition or disrupting the localization of the TJ [23–26]. The best known of these disruption methods

consists of a calcium switch from normal media concentrations to a low calcium environment, either by use of calcium-free media, or by chelation, resulting in endocytosis of the TJ.

Indeed, when A33-labeled LS174T cells were treated with 25 mM EGTA, a fraction of the surface A33 was endocytosed into intracellular compartments (Fig. 3a) similar to those observed for TJ proteins such as JAM-1, occludin, and ZO-1, and the adherens junction molecules β -catenin and E-cadherin [27]. As the various components of the TJ can be sorted into different compartments upon internalization, we also sought to determine the fate of endocytosed antigen. The internalization assay was modified such that LS174T cells were first A33-labeled and then tight-junction internalization was triggered by a calcium switch. Low calcium media was then replaced with fresh, calcium-containing media (washout), and recycled antibody-bound antigen was detected by binding of a secondary antibody (Fig. 3b, closed squares). The clear increase in secondary signal indicates that internalized antigen was able to return to the surface. In order to distinguish the relative contributions of resurfacing and possible new synthesis following the calcium switch, samples were also re-labeled with primary (open circles) following the incubation with secondary antibody. Recycling accounted for the bulk of overall signal increase, as opposed to additional primary labeling, which includes both new synthesis as well as replacement of primary label that may have dissociated during the course of the experiment.

Another behavior common to various IGSF proteins is a role in adhesion and subsequent establishment of barrier function—many A33 homologs participate in dimeric interactions involved in securing cell–cell contacts [28–31]. A number of viruses bind to IGSF proteins, even producing proteins that interfere with epithelial integrity by blocking these dimeric interactions [32]. We therefore investigated the ability of the clinical anti-A33 antibody to influence monolayer integrity as a means of accounting for the ability of the clinical antibody to penetrate tumors. One day after plating on a transwell insert, SW1222 cells were treated with either huA33 antibody or mouse anti-FLAG antibody as a control. In the presence of A33 antibody, the monolayer did not fully tighten, as evidenced by a decrease in electrical resistance, indicating a greater degree of leakiness of the tight junctions (Fig. 3c). This increased permeability not only connects A33 to other tight junction proteins and IGSF's, it implies a possible functional role in adhesion. Interestingly, when A33 antibodies were applied to fully formed monolayers, they were unable to increase permeability (data not shown), indicating that they lack the ability to actively pry open sealed junctions. This discrepant behavior may indicate that there is differential access to antigen between normal colon and tumors, which are known to possess disordered and leaky tight junctions [33,34].

Thus far, we have demonstrated that A33 antigen is partially colocalized with various TJ components, is internalized upon calcium switch, and antibodies to A33 can influence monolayer resistance. These results suggest a role for A33 at the TJ—an interesting possibility given the disorder of the TJ in cancer [33,35,36] and some of the proposed mechanisms by which A33 antibodies may gain tumor specific localization despite expression throughout the intestine. However, as the LS174T cells used did not form polarized monolayers, they are of limited utility in fully investigating the possibility that A33 is a component of the tight junction.

From a tumor-targeting perspective, these results are secondary to the unusual persistence of radiolabel in clinical patients, and the lack of internalization observed in cultured cells (Fig. 1). In fact, the results of the internalization assay hint at surface persistence that is longer lived than bulk membrane and accompanying proteins. In order to avoid capture and degradation during normal membrane turnover, we next supposed that there might be a tether actively stabilizing A33 in the membrane. Due to its colocalization with actin, and the actin-TJ linking protein ZO-1, the cytoskeleton was clearly implicated. Additionally, the cytoskeleton has been shown to regulate junction assembly and remodeling [37].

Accordingly, actin and microtubules were disrupted by treatment with either latrunculin B (Fig. 4a) or nocodazole (Fig. 4b). When A33-labeled cells were treated with these cytoskeleton-disrupting drugs, the antigen was internalized in a manner similar to the calcium switch—indicating that persistent surface localization requires intact cytoskeleton. Additionally, following a calcium switch, LS174T cells were washed into either normal media or media containing EGTA, nocodazole, or latrunculin, and at various time-points aliquots were removed, A33 labeled, and analyzed by flow cytometry (Fig. 4c). When EGTA was washed out and no drugs were washed in, the surface localization of A33 was restored. This restoration was blocked by disruption of the cytoskeleton.

Since many TJ proteins interact with the cytoskeleton and ZO-1 through a series of well-characterized binding domains, we looked for motifs within the A33 intracellular domain, which has been described as unusually acidic [6]. Upon closer inspection, a short region with high homology to occludin was found (Fig. 4d). Initially, this region of occludin was found to be required for TJ/membrane localization [38]. When the crystal structure of occludin was solved, it was found that this region acts as a hinge between two positively charged, acidic domains that are required for binding to ZO-1 [39]. Despite being otherwise non-homologous, the similarity between its intracellular domain and that of A33 are striking and point toward the possibility that they may have a common set of interactions with cytosolic proteins—most notably with the actin cytoskeleton, possibly through ZO-1.

As another means of assessing whether the A33 antigen is tethered on the membrane or part of a large protein complex such as the TJ, a series of photobleaching experiments was performed, in which the cell membrane was bleached at cell–cell junctions, and the recovery of either fluorescein-conjugated antibody-bound A33 or the membrane dye DiI was followed. The fluorescence of the membrane dye DiI had an almost complete recovery, while only 10% of A33 fluorescence was seen to recover over the course of 1 min (Fig. 5a). When observed over a longer period of time, A33 recovery was quite slow, and indicated that more than half of the antigen is immobile (Fig. 5b). This dramatic surface immobility corresponds quite well to other tight junction proteins, which have been studied in both cultured cells and live *drosophila* embryos [40,41].

The bleach geometry used prevents reporting of an accurate diffusivity value, as diffusivity is highly dependent on the area of the bleach region, which could not be precisely determined. However, since bleach areas were similar for both A33 and DiI, relative diffusivities can be reported. Excluding the immobile fraction, the diffusivity of complexed A33 was 2.5–3 orders of magnitude slower than that of DiI. As a second point of comparison, DiI recovery was compared to recovery of a CEACAM1-egfp fusion protein [16] in MCF-7 cells (data not shown). CEACAM1-egfp is known to reside in lipid rafts, but also to associate with actin through its short cytoplasmic domain [42,43]. Using the same bleach methodology, the diffusivity of CEACAM1, a distant homolog of A33, and a verified cell adhesion molecule, was found to be only fourfold slower than DiI.

As there was no significant difference between the recovery of A33 at regions of cell–cell contact and at regions of the membrane not associated with other cells (data not shown), this stability must not depend on trans interactions between cells at the TJ, and points toward either the incorporation of A33 antigen into a larger protein complex which is highly stabilized, or a more direct interaction with static regions of the cytoskeleton. Regardless of mechanism, an interaction with the cytoskeleton is consistent with our colocalization observations, homology, and the data demonstrating that the cytoskeleton is necessary for localization.

Additionally, since the persistence of label in clinical patients is the key feature of this antigen, we next determined the turnover half-life of antigen in cultured LS174T monolayers (Fig. 5c).

Monolayers were pulse-biotinylated and at various timepoints total protein was extracted. Biotinylated proteins were pulled down by incubating the lysate with streptavidin resin, and then cleaved from the resin by reduction of a disulfide bond. The resulting samples were run on an SDS-PAGE gel, transferred to nitrocellulose, and blotted to detect A33. Band intensities were quantified and fitted to an exponential decay. In this manner, the half-life of A33 was found to be 56 h. With a half-life of over 2 days, the A33 antigen is highly persistent relative to typical membrane proteins turnover times. For example, the turnover half-life for CEA in these same samples was found to be 15 h (M. Schmidt, unpublished). This long half-life is expected to be partially responsible for the sustained persistence of the therapeutic antibody to A33 in patients. Most significantly, this long half-life provides a strong motivation for further clinical study of the antigen as a target in PRIT.

Lastly, as there are a number of cell surface antigens with promise as targets in PRIT, we also directly compared A33 with what is perhaps the best studied of these antigens. Carcinoembryonic antigen (CEA) is a cell surface antigen that is frequently expressed at high levels at the apical surface of epithelial cells, and in a nonpolarized surface pattern in colon tumors [44]. Numerous studies have been performed targeting this well-characterized protein. As accessibility to chelated radionuclide is a key requirement for successful PRIT, we sought to compare the accessibility of antibody bound to A33 with CEA. Accordingly, LS174T cells were labeled with both an anti-A33 antibody (m100.310 Alexa*488) and an anti-CEA scFv (shMFE Alexa*594), and incubated at 37°C for 2 h prior to imaging. Intriguingly, after as short a period of 2 h, there is significant internalization of CEA, while A33 remains stably located at the cell surface, available to bind the radionuclide construct (Fig. 5d).

Taken together, these results demonstrate that the A33 antigen is a highly persistent, largely immobile, surface-localized protein. These findings help explain the unusual persistence of tumor associated anti-A33 antibodies in clinical trials, and indicate that the A33 antigen may have unique promise as a target in PRIT.

Discussion

A33 is a highly persistent surface-localized antigen. While the antigen is not cancer-specific, antibodies against A33 gain tumor specificity over the course of a week, possibly as the normal intestinal epithelium is shed. Most tumor cell lines tested showed little or no internalization of the antigen, both by immunofluorescent imaging of permeabilized and live, antibody-complexed cells, and in a flow-cytometric internalization assay which monitored accessibility to a secondary antibody. While initially surprising, as there had been reports that the antigen was internalized when bound by an antibody which recognizes a different epitope [22], this result is consistent with immunofluorescence images of resected colon tissue, in which the steady-state distribution of antigen is entirely on the cellular surface, with the possible exception of cells at the very tip of the crypt which are about to be shed (C. Chalouni, unpublished). The difference between these previous results [22] and those reported here are most likely due to differences in the methodology of detection of internalization or the particular cell lines examined. This phenotype may be reflected by the LIM1215 cell line, which unlike the rest of the lines tested, did internalize the antigen.

As a member of the immunoglobulin superfamily (IGSF) of proteins, which comprises a full 2% of the genome, A33 is a member of the largest class of mammalian proteins. Their basic extracellular structure consists of domains resembling the IgG fold, and they have notable diversity in their intracellular domains. Striking features of the A33 intracellular domain include a quadruple cysteine repeat followed by a highly acidic sequence. Its closest homologs include the coxsackie adenovirus receptor (CAR) [45], cortical thymocyte receptor (CTX) [45], endothelial cell adhesion molecule (ESAM), junction adhesion molecules 1–3 (JAM)

[46], and CEA-related cell adhesion molecules (CEACAMs) [47]. Many of these homologs have been implicated in cell–cell adhesion, and some are localized to regions of cell–cell contact or to the tight junction more specifically. They typically participate in dimeric interactions, and many also serve as attachment points for various intestinal viruses.

Here, we describe experiments that reveal some of the molecular properties of the A33 antigen. Taken together, this work demonstrates the persistent, immobile, and stable surface expression of A33—properties which may result from a link to the cytoskeleton through a complex of tight junction components. Additionally, these properties may be the source of the A33 antigen’s uniquely promising profile in clinical trials.

In the clinic, antibodies to A33 exhibit two distinctive properties. First, they remain tumor-localized for weeks. In some cases, persistent tumor localization is due to the residualizing properties of metal radionuclides. However, the A33 clinical trials have utilized radioactive iodine. Questions remain as to how these antibodies were able to persist— whether they were sequestered and stored along some trafficking route, or whether they simply remained bound to surface-localized antigen. Our studies here are consistent with the notion that the A33 antigen is surface-stabilized through a link to the cytoskeleton or as a part of a stable protein complex or membrane microdomain that allows the antigen to escape bulk membrane endocytosis and subsequent trafficking and endocytosis. The turnover half-life of greater than 2 days found here also likely underestimates the true turnover time in vivo. Over the course of the protocol used here, the cultures become overpopulated and some cells may respond by undergoing apoptosis, resulting in an artificially shorter half-life. Additionally, as mentioned previously, intracellular A33 staining is not seen in sections of human colon, except at the very tip of crypts, in cells that are proximal to being shed (C. Chalouni, unpublished). This data indicates that the simple explanation of persistence due to a lack of antigen turnover may be correct.

Secondly, and more significantly, antibodies to A33 were found to penetrate solid tumors [12]. The ability to penetrate solid tumors has proven to be a significant obstacle in RIT. To date, few successful RIT therapeutics target solid tumors. This failure is due to what are generally the conflicting goals of avoiding bone marrow toxicity while at the same time penetrating and thoroughly dosing tumor tissue. As a means to evade this toxicity at the same time as increasing penetration, manipulations of targeting construct size have been studied extensively. While these alterations do have the desired effect on clearance parameters, thorough tumor penetration has still proven an elusive goal.

The difficulty in localizing therapeutics to the core of tumors may be due to a consumption-based barrier to diffusion [51], in which antigen turnover reaches an equilibrium with diffusion and binding of the therapeutic at a given distance from the capillary—preventing penetration past that boundary. This phenomenon, which is further compounded by the “binding site barrier”, in which high affinity reagents bind to the first unoccupied antigen they encounter [48,49], works against deep tumor penetration. In the case of A33, perhaps this barrier is evaded as the antigen is not internalized and degraded on the time scale of diffusion [50].

The simple asset of persistent surface localization, which we have described here, may account for both of A33’s distinctive RIT properties. It may allow the clinical antibodies to gain tumor specificity as normal epithelium is shed, and to penetrate the core of a solid tumor as diffusion outpaces turnover. We likewise speculate that this surface persistence may allow antibodies to A33 to have high availability to a radionuclide construct in PRIT. Taken together, these results point to A33 as a candidate for two-step therapies.

Acknowledgments

The authors wish to kindly acknowledge funding by NCI CA101830, and the receipt of antibodies and cell lines from the Ludwig Institute and from Dr. John Shively at City of Hope.

References

1. DeNardo GL. Treatment of non-Hodgkin's lymphoma (NHL) with radiolabeled antibodies (mAbs). *Semin Nucl Med* 2005;35(3):202–211. [PubMed: 16098294]
2. Pagel JM, Hedin N, Subbiah K, Meyer D, Mallet R, Axworthy D, Theodore LJ, Wilbur DS, Matthews DC, Press OW. Comparison of anti-CD20 and anti-CD45 antibodies for conventional and pretargeted radioimmunotherapy of B-cell lymphomas. *Blood* 2003;101(6):2340–2348. [PubMed: 12446461]
3. Gruaz-Guyon A, Raguin O, Barbet J. Recent advances in pretargeted radioimmunotherapy. *Curr Med Chem* 2005;12(3):319–338. [PubMed: 15723622]
4. Boerman OC, van Schaijk FG, Oyen WJ, Corstens FH. Pretargeted radioimmunotherapy of cancer: progress step by step. *J Nucl Med* 2003;44(3):400–411. [PubMed: 12621007]
5. Johnstone CN, Tebbutt NC, Abud HE, White SJ, Stenvers KL, Hall NE, Cody SH, Whitehead RH, Catimel B, Nice EC, Burgess AW, Heath JK. Characterization of mouse A33 antigen, a definitive marker for basolateral surfaces of intestinal epithelial cells. *Am J Physiol Gastrointest Liver Physiol* 2000;279(3):G500–G510. [PubMed: 10960348]
6. Heath JK, White SJ, Johnstone CN, Catimel B, Simpson RJ, Moritz RL, Tu GF, Ji H, Whitehead RH, Groenen LC, Scott AM, Ritter G, Cohen L, Welt S, Old LJ, Nice EC, Burgess AW. The human A33 antigen is a transmembrane glycoprotein and a novel member of the immunoglobulin superfamily. *Proc Natl Acad Sci USA* 1997;94(2):469–474. [PubMed: 9012807]
7. Garin-Chesa P, Sakamoto J, Welt S, Real FX, Rettig WJ, Old LJ. Organ-specific expression of the colon cancer antigen A33, a cell surface target for antibody-based therapy. *Int J Oncol* 1996;9:465–471.
8. Welt S, Divgi CR, Real FX, Yeh SD, Garin-Chesa P, Finstad CL, Sakamoto J, Cohen A, Sigurdson ER, Kemeny N, et al. Quantitative analysis of antibody localization in human metastatic colon cancer: a phase I study of monoclonal antibody A33. *J Clin Oncol* 1990;8(11):1894–1906. [PubMed: 2230877]
9. Welt S, Divgi CR, Kemeny N, Finn RD, Scott AM, Graham M, Germain JS, Richards EC, Larson SM, Oettgen HF, et al. Phase I/II study of iodine 131-labeled monoclonal antibody A33 in patients with advanced colon cancer. *J Clin Oncol* 1994;12(8):1561–1571. [PubMed: 8040668]
10. Welt S, Scott AM, Divgi CR, Kemeny NE, Finn RD, Daghighian F, Germain JS, Richards EC, Larson SM, Old LJ. Phase I/II study of iodine 125-labeled monoclonal antibody A33 in patients with advanced colon cancer. *J Clin Oncol* 1996;14(6):1787–1797. [PubMed: 8656247]
11. Welt S, Ritter G, Williams C Jr, Cohen LS, John M, Jungbluth A, Richards EA, Old LJ, Kemeny NE. Phase I study of anticolon cancer humanized antibody A33. *Clin Cancer Res* 2003;9(4):1338–1346. [PubMed: 12684402]
12. Scott AM, Lee FT, Jones R, Hopkins W, MacGregor D, Cebon JS, Hannah A, Chong G, Paul U, Papenfuss A, Rigopoulos A, Sturrock S, Murphy R, Wirth V, Murone C, Smyth FE, Knight S, Welt S, Ritter G, Richards E, Nice EC, Burgess AW, Old LJ. A phase I trial of humanized monoclonal antibody A33 in patients with colorectal carcinoma: biodistribution, pharmacokinetics, and quantitative tumor uptake. *Clin Cancer Res* 2005;11(13):4810–4817. [PubMed: 16000578]
13. Chong G, Lee FT, Hopkins W, Tebbutt N, Cebon JS, Mountain AJ, Chappell B, Papenfuss A, Schleyer P, Paul U, Murphy R, Wirth V, Smyth FE, Potasz N, Poon A, Davis ID, Saunderson TJ, O'Keefe G, Burgess AW, Hoffman EW, Old LJ, Scott AM. Phase I trial of 131I-huA33 in patients with advanced colorectal carcinoma. *Clin Cancer Res* 2005;11(13):4818–4826. [PubMed: 16000579]
14. Ritter G, Cohen LS, Williams C Jr, Richards EC, Old LJ, Welt S. Serological analysis of human anti-human antibody responses in colon cancer patients treated with repeated doses of humanized monoclonal antibody A33. *Cancer Res* 2001;61(18):6851–6859. [PubMed: 11559561]
15. Johnstone CN, White SJ, Tebbutt NC, Clay FJ, Ernst M, Biggs WH, Viars CS, Czekay S, Arden KC, Heath JK. Analysis of the regulation of the A33 antigen gene reveals intestine-specific mechanisms of gene expression. *J Biol Chem* 2002;277(37):34531–34539. [PubMed: 12114523]

16. Chen CJ, Shively JE. The cell–cell adhesion molecule carcinoembryonic antigen-related cellular adhesion molecule 1 inhibits IL-2 production and proliferation in human T cells by association with Src homology protein-1 and down-regulates IL-2 receptor. *J Immunol* 2004;172(6):3544–3552. [PubMed: 15004155]
17. Ellenberg J, Siggia ED, Moreira JE, Smith CL, Presley JF, Worman HJ, Lippincott-Schwartz J. Nuclear membrane dynamics and reassembly in living cells: targeting of an inner nuclear membrane protein in interphase and mitosis. *J Cell Biol* 1997;138(6):1193–1206. [PubMed: 9298976]
18. Umenishi F, Verbavatz JM, Verkman AS. cAMP regulated membrane diffusion of a green fluorescent protein-aquaporin 2 chimera. *Biophys J* 2000;78(2):1024–1035. [PubMed: 10653816]
19. Partikian A, Olveczky B, Swaminathan R, Li Y, Verkman AS. Rapid diffusion of green fluorescent protein in the mitochondrial matrix. *J Cell Biol* 1998;140(4):821–829. [PubMed: 9472034]
20. Le TL, Yap AS, Stow JL. Recycling of E-cadherin: a potential mechanism for regulating cadherin dynamics. *J Cell Biol* 1999;146(1):219–232. [PubMed: 10402472]
21. Ji H, Moritz RL, Reid GE, Ritter G, Catimel B, Nice E, Heath JK, White SJ, Welt S, Old LJ, Burgess AW, Simpson RJ. Electrophoretic analysis of the novel antigen for the gastrointestinal-specific monoclonal antibody, A33. *Electrophoresis* 1997;18(3–4):614–621. [PubMed: 9150949]
22. Daghighian F, Barendswaard E, Welt S, Humm J, Scott A, Willingham MC, McGuffie E, Old LJ, Larson SM. Enhancement of radiation dose to the nucleus by vesicular internalization of iodine-125-labeled A33 monoclonal antibody. *J Nucl Med* 1996;37(6):1052–1057. [PubMed: 8683300]
23. Bruewer M, Utech M, Ivanov AI, Hopkins AM, Parkos CA, Nusrat A. Interferon-gamma induces internalization of epithelial tight junction proteins via a macropinocytosis-like process. *Faseb J* 2005;19(8):923–933. [PubMed: 15923402]
24. Kevil CG, Oshima T, Alexander B, Coe LL, Alexander JS. H(2)O(2)-mediated permeability: role of MAPK and occludin. *Am J Physiol Cell Physiol* 2000;279(1):C21–C30. [PubMed: 10898713]
25. Harhaj NS, Antonetti DA. Regulation of tight junctions and loss of barrier function in pathophysiology. *Int J Biochem Cell Biol* 2004;36(7):1206–1237. [PubMed: 15109567]
26. Musch MW, Walsh-Reitz MM, Chang EB. Roles of ZO-1, occludin, and actin in oxidant-induced barrier disruption. *Am J Physiol Gastrointest Liver Physiol* 2006;290(2):G222–G231. [PubMed: 16239402]
27. Ivanov AI, Nusrat A, Parkos CA. Endocytosis of epithelial apical junctional proteins by a clathrin-mediated pathway into a unique storage compartment. *Mol Biol Cell* 2004;15:176–188. [PubMed: 14528017]
28. Mandell KJ, Parkos CA. The JAM family of proteins. *Adv Drug Deliv Rev* 2005;57(6):857–867. [PubMed: 15820556]
29. Gray-Owen SD, Blumberg RS. CEACAM1: contact-dependent control of immunity. *Nat Rev Immunol* 2006;6(6):433–446. [PubMed: 16724098]
30. Kostrewa D, Brockhaus M, D’Arcy A, Dale GE, Nelboeck P, Schmid G, Mueller F, Bazzoni G, Dejana E, Bartfai T, Winkler FK, Hennig M. X-ray structure of junctional adhesion molecule: structural basis for homophilic adhesion via a novel dimerization motif. *Embo J* 2001;20(16):4391–4398. [PubMed: 11500366]
31. Brummendorf T, Lemmon V. Immunoglobulin superfamily receptors: cis-interactions, intracellular adapters and alternative splicing regulate adhesion. *Curr Opin Cell Biol* 2001;13(5):611–618. [PubMed: 11544031]
32. Walters RW, Freimuth P, Moninger TO, Ganske I, Zabner J, Welsh MJ. Adenovirus fiber disrupts CAR-mediated intercellular adhesion allowing virus escape. *Cell* 2002;110(6):789–799. [PubMed: 12297051]
33. Mullin JM, Agostino N, Rendon-Huerta E, Thornton JJ. Keynote review: epithelial and endothelial barriers in human disease. *Drug Discov Today* 2005;10(6):395–408. [PubMed: 15808819]
34. Sawada N, Murata M, Kikuchi K, Osanai M, Tobioka H, Kojima T, Chiba H. Tight junctions and human diseases. *Med Electron Microsc* 2003;36(3):147–156. [PubMed: 14505058]
35. Mullin JM. Epithelial barriers, compartmentation, and cancer. *Sci STKE* 2004;216:pe2.
36. Soler AP, Miller RD, Laughlin KV, Carp NZ, Klurfeld DM, Mullin JM. Increased tight junctional permeability is associated with the development of colon cancer. *Carcinogenesis* 1999;20(8):1425–1431. [PubMed: 10426787]

37. Ivanov AI, McCall IC, Babbin B, Samarin SN, Nusrat A, Parkos CA. Microtubules regulate disassembly of epithelial apical junctions. *BMC Cell Biol* 2006;7:12. [PubMed: 16509970]
38. Furuse M, Itoh M, Hirase T, Nagafuchi A, Yonemura S, Tsukita S, Tsukita S. Direct association of occludin with ZO-1 and its possible involvement in the localization of occludin at tight junctions. *J Cell Biol* 1994;127(6):1617–1626. [PubMed: 7798316]
39. Li Y, Fanning AS, Anderson JM, Lavie A. Structure of the conserved cytoplasmic C-terminal domain of occludin: identification of the ZO-1 binding surface. *J Mol Biol* 2005;352:151–164. [PubMed: 16081103]
40. Cliffe A, Mieszczynek J, Bienz M. Intracellular shuttling of a *Drosophila* APC tumour suppressor homolog. *BMC Cell Biology* 2004;5:37. [PubMed: 15458577]
41. Thomas T, Jordan K, Simek J, Shao Q, Jedescko C, Walton P, Laird DW. Mechanisms of Cx43 and Cx26 transport to the plasma membrane and gap junction regeneration. *J Cell Sci* 2005;119:4451–4462. [PubMed: 16159960]
42. Kirshner J, Schumann D, Shively JE. CEACAM1, a cell–cell adhesion molecule, directly associates with annexin II in a three-dimensional model of mammary morphogenesis. *J Biol Chem* 2003;278(50):50338–50435. [PubMed: 14522961]
43. Schumann D, Chen CJ, Kaplan B, Shively JE. Carcinoembryonic antigen cell adhesion molecule 1 directly associates with cytoskeleton proteins actin and tropomyosin. *J Biol Chem* 2001;276(50):47421–47433. [PubMed: 11595750]
44. Hammarstrom S. The carcinoembryonic antigen (CEA) family: structures, suggested functions and expression in normal and malignant tissues. *Semin Cancer Biol* 1999;9(2):67–81. [PubMed: 10202129]
45. Chretien I, Marcuz A, Courtet M, Katevuo K, Vainio O, Heath JK, White SJ, Du Pasquier L. CTX, a *Xenopus thymocyte* receptor, defines a molecular family conserved throughout vertebrates. *Eur J Immunol* 1998;28(12):4094–4104. [PubMed: 9862345]
46. Bazzoni G. The JAM family of junctional adhesion molecules. *Curr Opin Cell Biol* 2003;15(5):525–530. [PubMed: 14519386]
47. Kuespert K, Pils S, Hauck CR. CEACAMs: their role in physiology and pathophysiology. *Curr Opin Cell Biol* 2006;18:565–571. [PubMed: 16919437]
48. van Osdol W, Fujimori K, Weinstein JN. An analysis of monoclonal antibody distribution in microscopic tumor nodules: consequences of a “binding site barrier”. *Cancer Res* 1991;51(18):4776–4784. [PubMed: 1893370]
49. Saga T, Neumann RD, Heya T, Sato J, Kinuya S, Le N, Paik CH, Weinstein JN. Targeting cancer micrometastases with monoclonal antibodies: a binding-site barrier. *Proc Natl Acad Sci USA* 1995;92(19):8999–9003. [PubMed: 7568060]
50. Graff CP, Wittrup KD. Theoretical analysis of antibody targeting of tumor spheroids: importance of dosage for penetration, and affinity for retention. *Cancer Res* 2003;63(6):1288–1296. [PubMed: 12649189]
51. Thurber GM, Zajic SC, Wittrup KD. Theoretic criteria for antibody penetration into solid tumors and micrometastases. *J Nucl Med* 2007;48(6):995–999. [PubMed: 17504872]

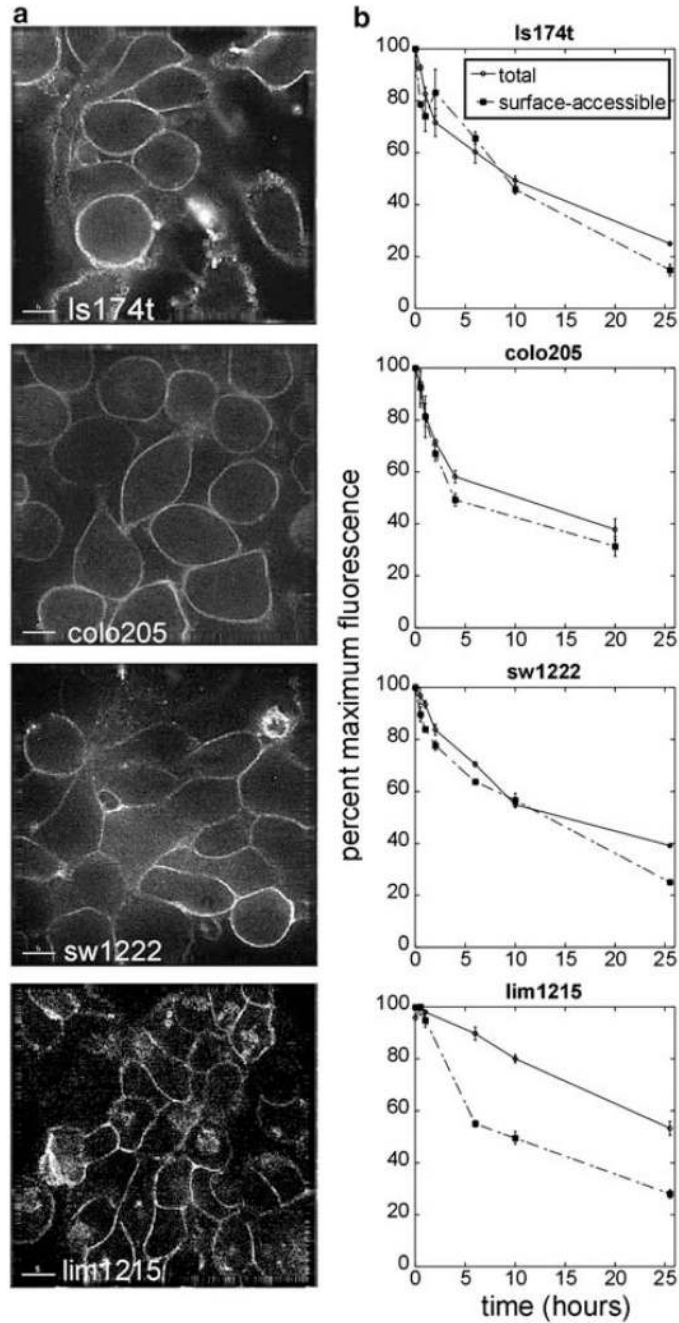


Fig. 1.

Distribution of antibody-bound A33 antigen. **a** Cultured colon tumor epithelial cells contain little intracellular A33 antigen. Each of four cell lines were grown on coverslips, fixed, permeabilized, and A33 antigen was labeled with the monoclonal antibody m100.310*Alexa 488. Internal pools of antigen were seen only in LIM1215 cells. *Bar* represents 5 μm . **b** Antibody-bound A33 antigen shows persistent surface localization in a flow cytometric assay of dynamic internalization kinetics. Suspended cells were A33-labeled at 0°C and then incubated at 37°C, allowing labeled antigen to be internalized. After shifting cultures to 37°C, aliquots were removed and labeled with anti-mouse PE and analyzed flow cytometry in order to determine the fraction of labeled A33 that remained surface accessible over time. The level

of surface-accessible A33 did not fall significantly below the level of total A33, indicating little internalization of the antibody-bound antigen in all cell lines tested except LIM1215. The decrease in total A33 signal is likely due to dissociation of the primary antibody, as the antigen is not shed

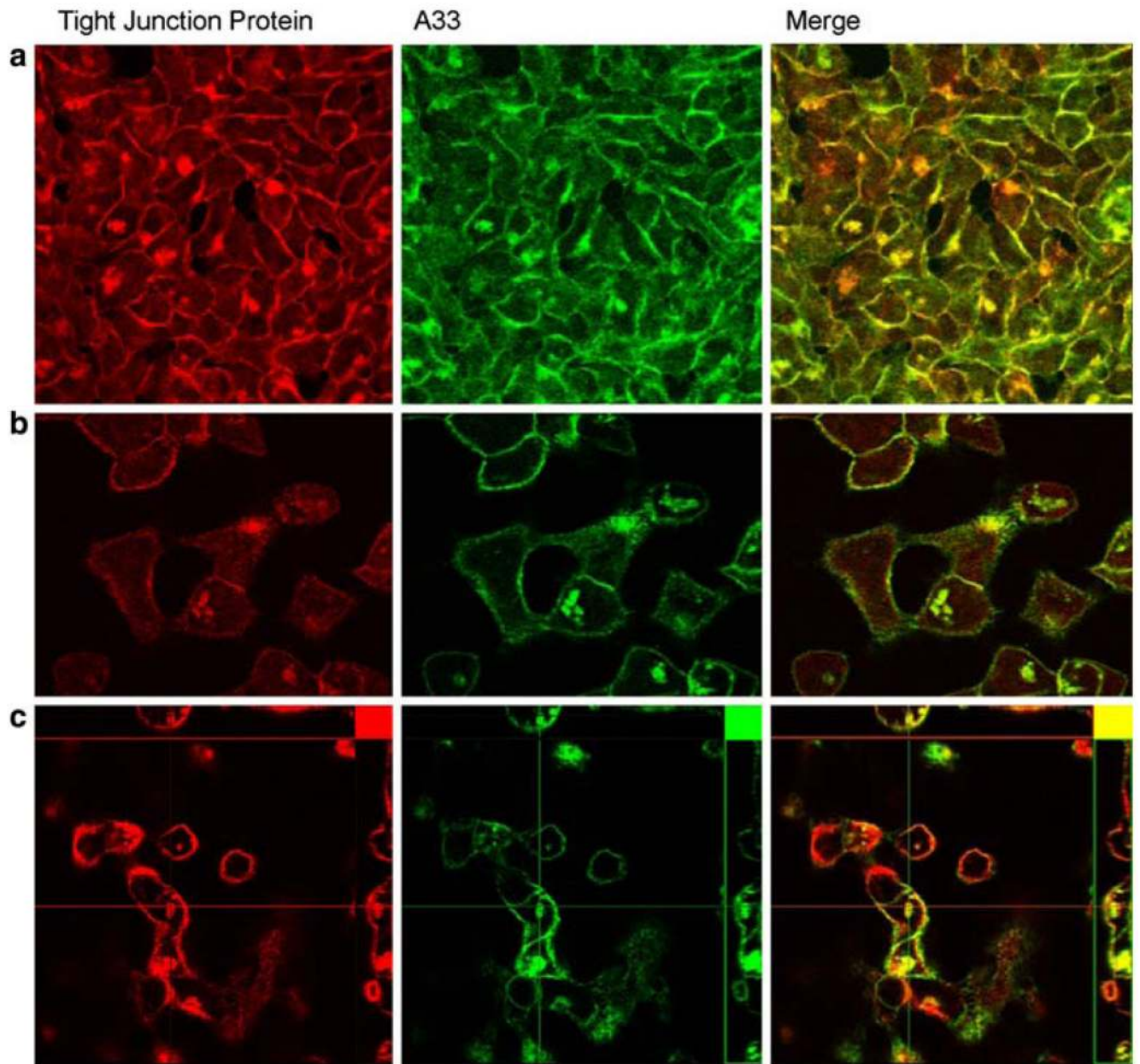
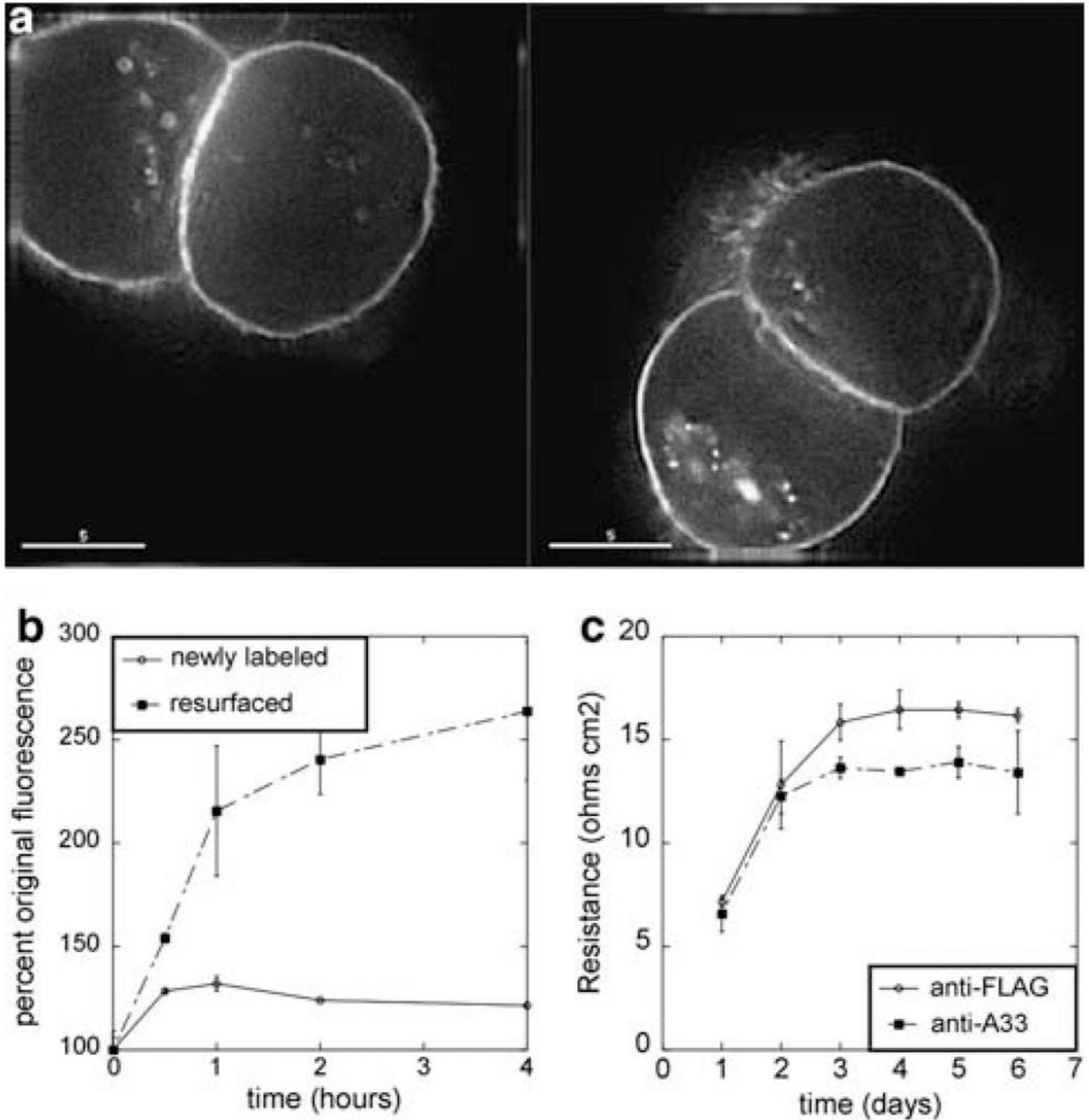


Fig. 2. Colocalization profile of A33 antigen. Tight junction proteins are false-colored in red, and A33 antigen in *green*. **a** A33 partially colocalizes with the tight junction protein occludin. Immunofluorescence image of LIM1215 cells showing colocalization of A33 antigen and occludin. **b** A33 partially colocalizes with the actin-binding, tight junction-associated protein, ZO-1. Immunofluorescence image of LIM1215 cells showing colocalization of A33 antigen and ZO-1. **c** A33 partially colocalizes with the cytoskeleton. Immunofluorescence image of LIM1215 cells showing colocalization of A33 antigen and actin. Images have been false-colored for clarity

**Fig. 3.**

Investigation of A33 as a tight junction-associated protein. **a** Calcium chelation triggers A33 internalization. LS174T cells were labeled with m100.310*Alexa 488, and culture media was treated with 25 mM EGTA to chelate calcium. At 2 h, there were clear intracellular pools of antigen, a phenomenon common to junction-associated proteins. **b** Replacement of calcium restores A33 surface localization. When EGTA is washed out, previously labeled A33 returns to the surface. Cell aliquots were labeled with m100.310*Alexa 488 and then treated with EGTA for 2 h. Following media replacement, aliquots were removed and labeled with a secondary-PE conjugate, and then again with m100.310*Alexa 488, and subjected to flow cytometry. **c** Anti-A33 antibody decreases monolayer integrity. SW1222 cells were grown on

transwell inserts, treated with antibodies 1 day after plating, and transepithelial electrical resistance was measured across the monolayer

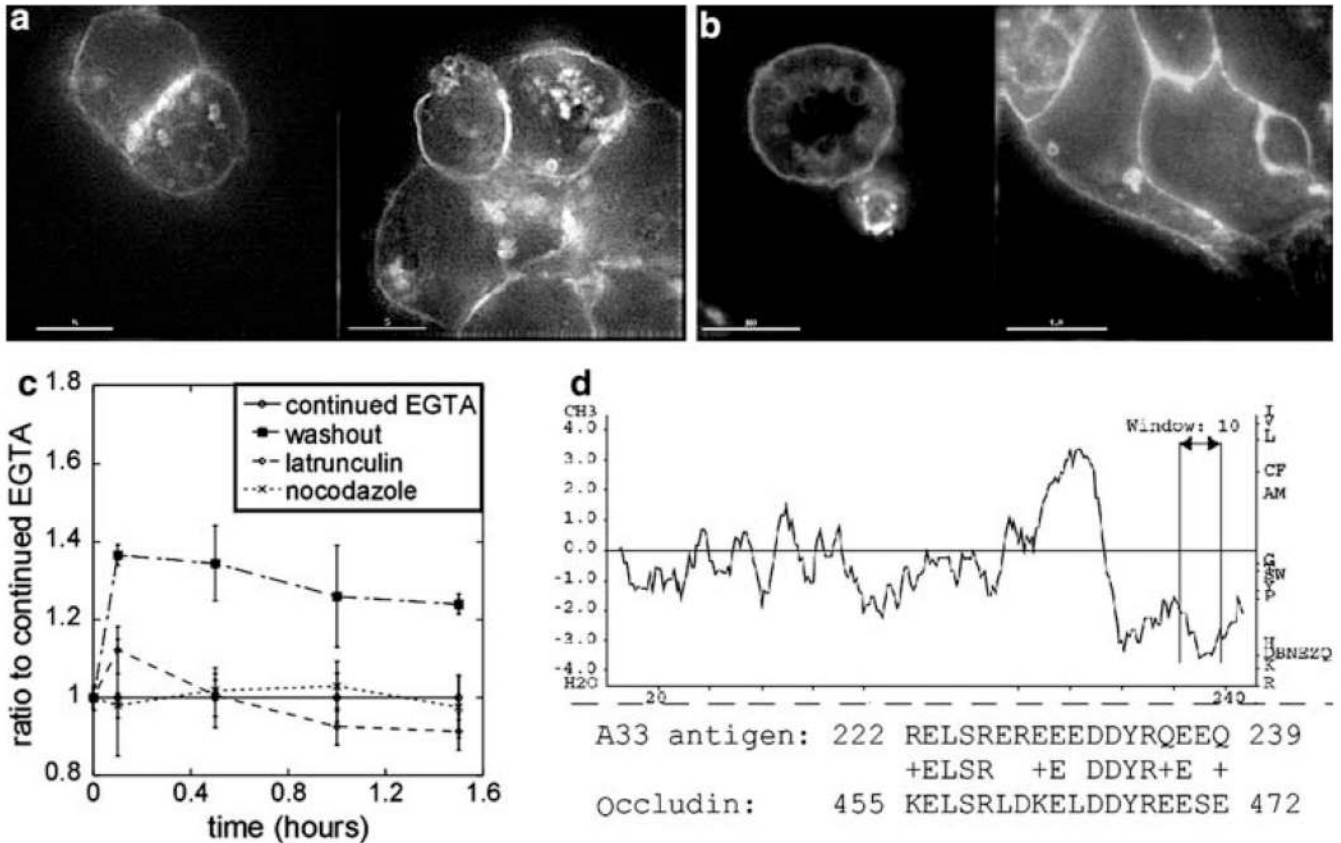


Fig. 4. Determination of the role of cytoskeleton in A33 localization. **a** Effect of disrupting actin on antigen distribution. Immunofluorescence images of A33-labeled LS174T cells after treatment with 100 nM latrunculin B for 2 h demonstrates internalization. **b** Effect of disrupting microtubules on antigen distribution. Immunofluorescence images of A33-labeled LS174T cells after treatment with 50 μ M nocodazole for 2 h demonstrates internalization. **c** Disruption of the cytoskeleton prevents recovery of surface-expressed A33. LS174T cells were labeled and then incubated with EGTA. Following internalization, media was exchanged with either fresh media (washout), or fresh media containing latrunculin, nocodazole, or EGTA (continued EGTA). Surface localization was restored only in cells with intact cytoskeleton and normal calcium levels. **d** Possible functional homology between A33 and occludin intracellular domains. A33 and occludin share a highly acidic intracellular region and a negatively charged hinge found to be important for TJ localization. Hydrophobicity plot of A33 antigen, detailing the hinge region with high homology to occludin

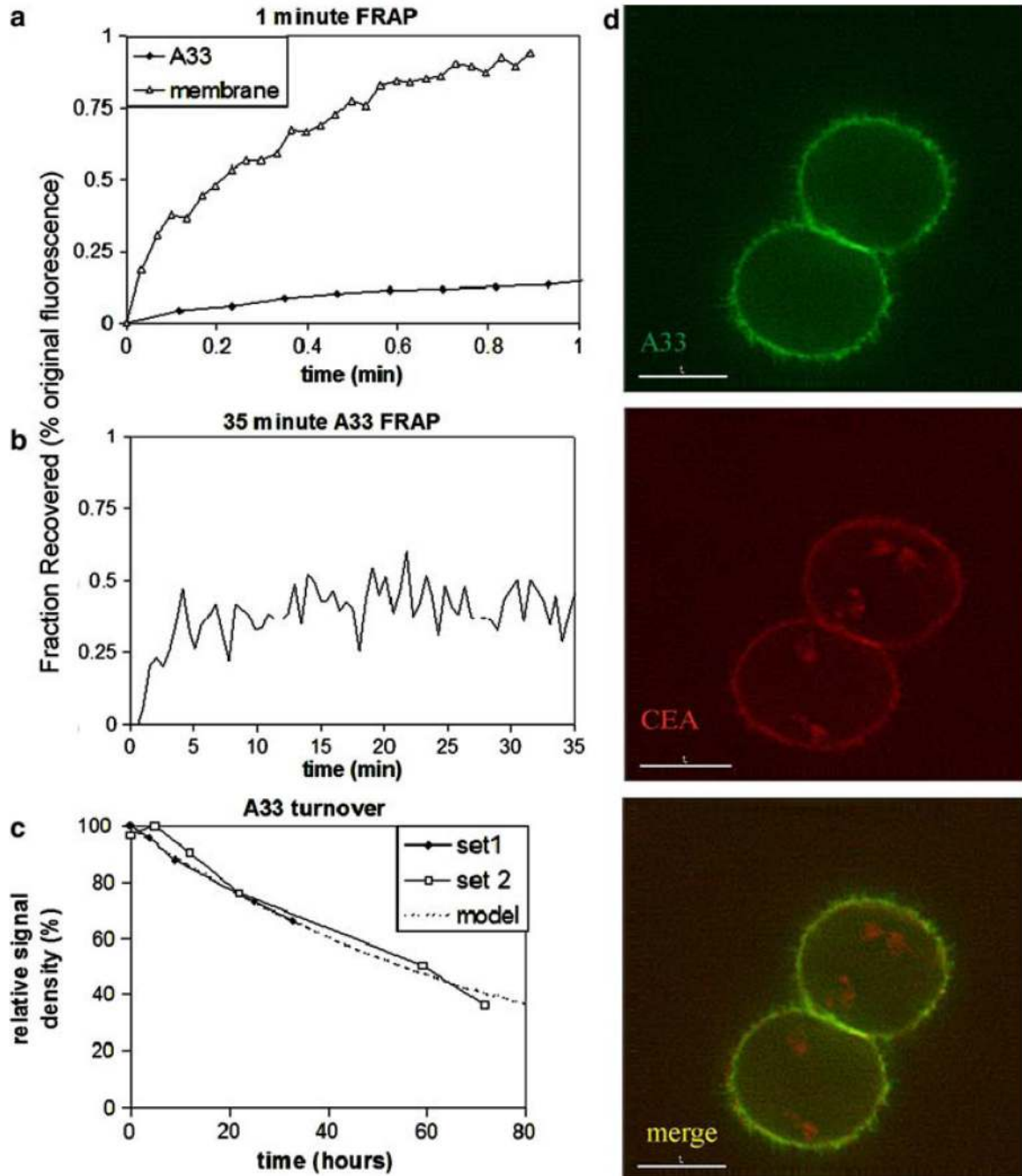


Fig. 5. Determination of the mobility and persistence of antibody-bound A33. **a** Over the course of 1 min, bleached plasma membrane has a near full recovery of fluorescence while very little A33 fluorescence recovers. Fraction of fluorescence recovered over time for bleached m100.310 antibody bound to A33 and the plasma membrane marker DiI. ($N = 8$, LS174T cells). **b** Even over much longer time scales, antibody-bound A33 fluorescence recovery is slow and incomplete. 35-min time course of antibody bound to A33 after photobleaching. ($N = 6$, LS174T cells). **c** The A33 antigen is persistent, having a surface expression halflife of 56 h in cultured monolayers. Cell surface proteins of cultured LS174T cells were pulse-biotinylated, extracted, and pulled down with streptavidin beads. The precipitated proteins were reduced off

the beads, subjected to gel electrophoresis and blotted to detect A33 antigen. Signal intensity of two data sets is plotted against time post-biotinylation, and fit to an exponential decay. **d** While other immunotherapy targets are internalized, A33 antigen remains on the surface. LS174T cells were labeled with both m100.310*Alexa 488 and anti-CEA shMFE*594 for 2 h at 37°C before imaging on a deconvolution microscope